PAPER • OPEN ACCESS

Directing folding pathways for multi-component DNA origami nanostructures with complex topology

To cite this article: A E Marras *et al* 2016 *New J. Phys.* **18** 055005

View the article online for updates and enhancements.

Related content

- Competitive annealing of multiple DNA origami: formation of chimeric origami
  Jacob M Majikes, Jessica A Nash and Thomas H LaBean

- Effect of anchor positioning on binding and diffusion of elongated 3D DNA nanostructures on lipid membranes
  Alena Khmelinskaia, Henri G Franquelim, Eugene P Petrov et al.

- Sub-10 nm patterning with DNA nanostructures: a short perspective
  Ke Du, Myeongkee Park, Junjun Ding et al.

Recent citations

- Co-self-assembly of multiple DNA origami nanostructures in a single pot
  Joshua A. Johnson *et al*

- DNA origami
  Swarup Dey *et al*

- MrDNA: a multi-resolution model for predicting the structure and dynamics of DNA systems
  Aleksei Aksimentiev and Christopher Maffeo

New Journal of Physics

The open access journal at the forefront of physics

CrossMark

PAPER

Directing folding pathways for multi-component DNA origami nanostructures with complex topology

A E Marras[1], L Zhou[1], V Kolliopoulos[2], H-J Su[1] and C E Castro[1,3]

[1] Department of Mechanical and Aerospace Engineering, The Ohio State University, Columbus, OH 43210, USA
[2] Department of Chemical and Biomolecular Engineering, The Ohio State University, Columbus, OH 43210, USA
[3] Biophysics Graduate Program, The Ohio State University, Columbus, OH 43210, USA

E-mail: castro.39@osu.edu

Abstract

Molecular self-assembly has become a well-established technique to design complex nanostructures and hierarchical mesoscale assemblies. The typical approach is to design binding complementarity into nucleotide or amino acid sequences to achieve the desired final geometry. However, with an increasing interest in dynamic nanodevices, the need to design structures with motion has necessitated the development of multi-component structures. While this has been achieved through hierarchical assembly of similar structural units, here we focus on the assembly of topologically complex structures, specifically with concentric components, where post-folding assembly is not feasible. We exploit the ability to direct folding pathways to program the sequence of assembly and present a novel approach of designing the strand topology of intermediate folding states to program the topology of the final structure, in this case a DNA origami slider structure that functions much like a piston-cylinder assembly in an engine. The ability to program the sequence and control orientation and topology of multi-component DNA origami nanostructures provides a foundation for a new class of structures with internal and external moving parts and complex scaffold topology. Furthermore, this work provides critical insight to guide the design of intermediate states along a DNA origami folding pathway and to further understand the details of DNA origami self-assembly to more broadly control folding states and landscapes.

Introduction

Directing order of assembly and orientation of components is crucial in manufacturing across multiple scales, in particular for topologically complex assemblies where components must fit inside or around other components in specific orientations. Traditionally this is achieved by temporal and spatial control of assembly where components are fabricated individually and then assembled by direct manipulation. This type of multi-stage assembly with controlled component orientation is often an essential part of manufacturing complex machines with moving components that interact [1]. For example, in an engine, the crank-shaft and piston must be directionally inserted into cylinder bores in the engine block prior to closing and sealing the engine assembly. While self-assembly has become an increasingly promising approach for manufacturing at multiple length scales, the ability to program self-assembly processes with controlled fabrication sequence and topology for multi-component nanostructures is a major challenge especially at the molecular scale where random thermal fluctuations are an integral part of the fabrication process.

For complex multi-component nanodevices, controlling the sequence of component assembly and the component orientation during the assembly process may be critical to achieve the desired structure and improve yield. The concept of considering assembly in the design process is well-established for macroscopic systems and is referred to as Design for Manufacture and Assembly (DFMA) [2]. Fundamental research on mechanical

assembly sequence analysis provides important guidelines on how the order of assembly affects the assembly efficiency [3] and how to select an optimal assembly sequence. Furthermore, constraint analysis studies show that appropriately constraining the motions of a component in selected directions can significantly improve the assembly efficiency (success rate), in particular for kinematic assemblies with moving components. In this work, we integrate concepts inspired by DFMA including controlling assembly sequence and orienting components during assembly that can greatly improve the assembly efficiency.

Since our fabrication process relies on self-assembly, the sequence and orientation of assembly cannot be controlled by direct manipulation. Recent work at larger scales has established automated control of fabrication sequence and orientation in macroscopic systems using shape memory materials to program the self-assembly of complex containers [4], 2D sheets [5] and robots [6]. These approaches rely on folding creases in 2D sheets, which is not directly applicable to most molecular systems. In biomolecular nanotechnology, temporally programmed self-assembly has generally been approached by hierarchical assembly of similar units to construct polyhedra [7–9], 1D arrays [10–13], 2D lattices or crystals [14–16] and 3D crystals [17]. The hierarchical assembly of similar units has also been widely explored for colloidal nanoparticles [18].

In contrast to the repetition of relatively simple geometric units, the scaffolded DNA origami approach [19–21] is a robust method for fabricating DNA nanostructures with unprecedented geometry complexity [22]. Recent advances exhibit a push towards increasingly intricate geometries [23] including cages [8, 24], containers [20, 25, 26], dynamic devices with constrained motion [27–33], and more [11, 34–36]. One recent study developed a multi-component dynamic device by folding individual components and then assembling them in multiple reaction steps [37]. Here we establish methods to fabricate multi-component dynamic devices of comparable complexity in a single reaction step by developing design strategies to program multi-stage self-assembly in a one-pot folding reaction. Although the details of the self-assembly process are not yet well understood, previous studies of scaffolded DNA origami self-assembly have revealed it is a highly cooperative process [38–40] where folding of structures or components can occur at a single temperature [39]. A recent study [41] further demonstrated the presence of competing folding pathways and the ability to bias a particular pathway for a flat rectangular DNA origami structure.

Building on these prior studies, this work demonstrates the ability to direct folding pathways in the multi-stage one-pot assembly of a DNA origami nanostructure with multiple components arranged in complex topology. In particular, the basis of this study is a DNA origami 'slider' structure, first presented in 2015 [28], that comprises two concentrically arranged components that undergo relative sliding motion. Here we present a novel study of directing folding pathways to control order of fabrication and structure topology during self-assembly. The assembly landscape for the DNA origami slider is illustrated in figure 1. We exploit the cooperativity of DNA origami assembly to fold the components in sequence and modify the design of the constituent DNA strands to control the order of folding. We further establish a strategy for making tight-fitting concentric structures that relies on designing the scaffold topology of the intermediate state where only one out of the two components is folded. Finally, we present a novel approach to actuate the fully folded slider into a contracted or extended configuration.

Methods

DNA origami nanostructure design

Our DNA origami slider is comprised of two stiff components, an inner cylinder and an outer tube, that are connected together via flexible scaffold DNA connections that allow relative translational motion. The nanostructures were designed from a single 8064 nt scaffold in the custom design software cadnano [42]. All cadnano designs and staple sequences are provided in figures S1–S12 in the supplemental information and tables S1–S12 provided in a supplemental file. The inner cylinder comprises a backstop with 42–44 double-stranded DNA helices in the cross-section and a 6-helix bundle with a diameter of ~6 nm extended from the center of the backstop that serves as the track for sliding motion. The outer tube has 30 double-stranded DNA helices in the cross-section with a maximum outside diameter of ~18 nm and a minimum inside diameter of ~10 nm, leaving an average gap between the inner track and outer tube of ~2 nm.

We designed a number of versions of our structure to test the hypothesis that reaching the concentrically folded final structure required a specific folding pathway, namely first folding the inside track, and then folding the outer tube directly around the track since inserting the track into the tube after both are folded is likely highly challenging. Building on previous studies of DNA origami self-assembly [38, 39, 41] we aimed to fold the inner track component first by designing the constituent staples so they would anneal at higher temperatures, which occur early in the thermal annealing ramp. Specifically, staple cross-overs were selectively removed to create thermodynamically stable binding sites at locations where it was desired to initiate folding (figure S13). We also designed versions of the slider structure where the staples were modified to initiate folding on the outer tube

Figure 1. Assembly landscape for multi-component DNA origami slider. The raw materials including the scaffold and the staples for each component are single-stranded at high temperatures (left). The initial folding trajectory (initiating folding with the track or the tube) during annealing is determined by the thermodynamics of staple binding, which can be controlled by the staple design. Due to the cooperativity of DNA origami assembly, folding of one component proceeds to completion prior to folding the second component. We force the track to fold first by increasing the local binding energy of its staples. Once the first component is folded, the second component then folds so the structure assembles either in the concentric or non-concentric state. We hypothesize that the complex topology of the concentric state can be achieved by folding the track component first, and exploiting the intermediate state to pre-arrange the tube scaffold around the track in the intermediate state. Once the slider is assembled the energy barrier to excessively extend the slider prevents switching between the concentric and non-concentric states.

component first for control experiments. We then designed several 'track first' slider structures with varying scaffold topology in the intermediate state (only the inside track is folded). All design versions are depicted and labeled in figures S1–S12.

DNA origami fabrication and characterization

Staple sequences were output from cadnano designs (tables S1–S12) and were obtained from a commercial vendor (Eurofins, Huntsville, AL). The scaffold was produced in our lab as previously described [21]. The DNA sliders were fabricated using standard DNA origami folding procedures [21]. Briefly, the standard folding process involves mixing the scaffold at 20 nM (black DNA template in figure 2, top left) with a 10-fold excess of 161–186 synthesized oligonucleotides called 'staples' (colored strands in figure 2) into a folding reaction containing 1 mM EDTA, 5 mM NaCl, 5 mM Tris, and 18 mM $MgCl_2$. This mixture was then subjected to a thermal annealing ramp consisting of a short melting phase ($\sim$65 °C) for $\sim$2 h, followed by a slow anneal down to 25 °C at a rate of 3 h /°C. Additional thermal annealing ramps were performed to probe intermediate states of folding as described subsequently. After annealing, self-assembly results were evaluated by agarose gel electrophoresis as previously described [21].

Transmission electron microscopy (TEM) analysis of nanostructures

Samples were prepared for TEM as previously described in [28, 30]. Briefly, samples were deposited onto copper grids with a formvar/copper film (EMS, Hatfield, PA). After deposition the samples were washed and then stained with a 2% Uranyl-Formate stain solution with 25 mM NaOH. Samples were imaged at the Campus Microscopy and Imaging Facility on a FEI Tecnai G2 Spirit TEM at an acceleration voltage of 80 kV as well as at the Center for Electron Microscopy and Analysis on a FEI Tecnai F20 TEM at 200 kV, both located at The Ohio State University.

Conformational analysis of slider structures was performed manually from TEM images to evaluate fraction of concentric structures. Sample TEM images are available in figures S14–S27. The length of the sliders was also measured manually using the software ImageJ. Only structures with clearly visible track and tube were included in the analyses. Additionally, only concentrically folded structures were considered when measuring extension. Analysis of measurement error is available in figure S28 and shows a standard deviation of 0.95 nm. Extension distributions were created and analyzed in MATLAB.

Probing folding pathways and intermediate states of folding

To probe intermediate states of folding, we developed folding and characterization protocols modified from a previous study focused on constant temperature folding of DNA origami [39]. Specifically, we ran partial folding
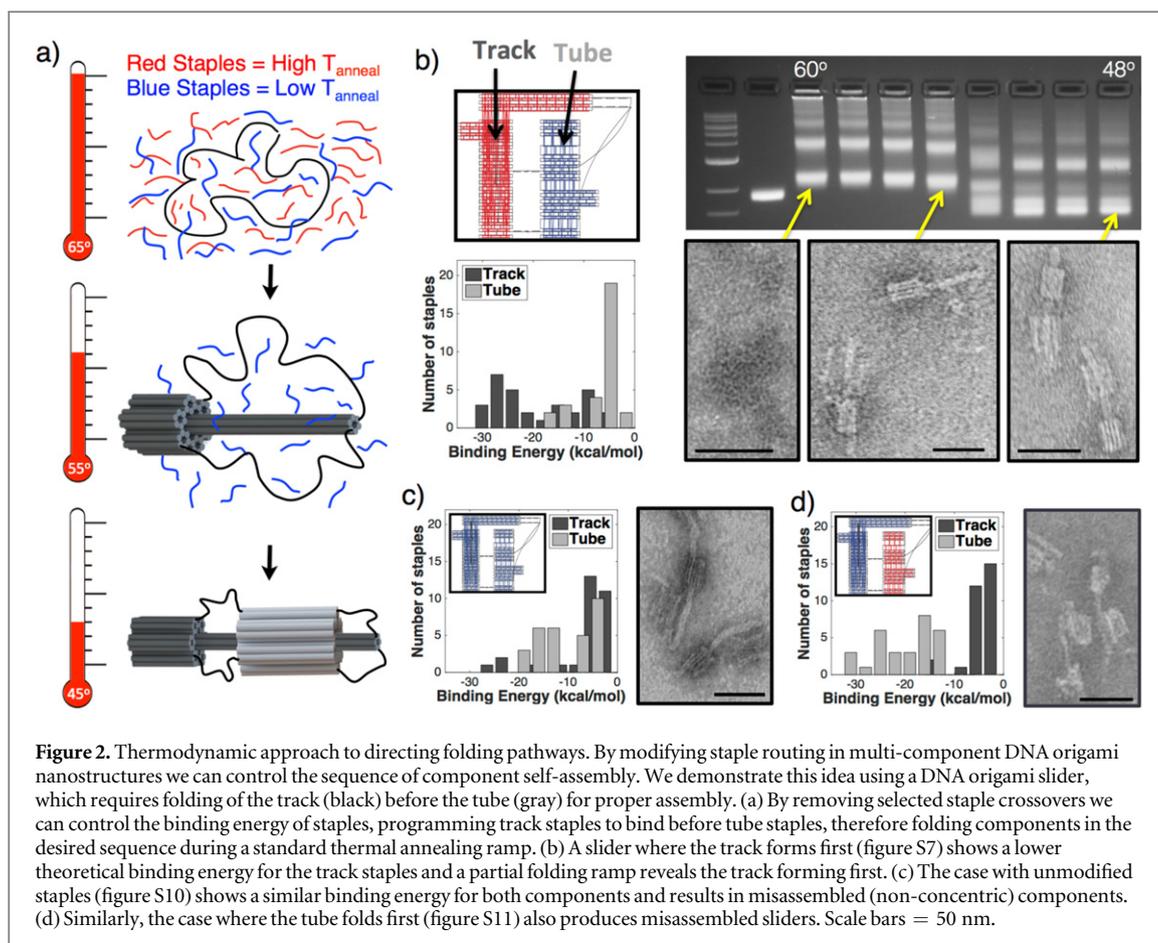
Figure 2. Thermodynamic approach to directing folding pathways. By modifying staple routing in multi-component DNA origami nanostructures we can control the sequence of component self-assembly. We demonstrate this idea using a DNA origami slider, which requires folding of the track (black) before the tube (gray) for proper assembly. (a) By removing selected staple crossovers we can control the binding energy of staples, programming track staples to bind before tube staples, therefore folding components in the desired sequence during a standard thermal annealing ramp. (b) A slider where the track forms first (figure S7) shows a lower theoretical binding energy for the track staples and a partial folding ramp reveals the track forming first. (c) The case with unmodified staples (figure S10) shows a similar binding energy for both components and results in misassembled (non-concentric) components. (d) Similarly, the case where the tube folds first (figure S11) also produces misassembled sliders. Scale bars = 50 nm.

ramps where annealing was stopped at different points during the thermal ramp. To facilitate multiplexed analysis, these folding reactions were run in parallel using a temperature gradient across a 48-well block of a C1000 Thermo cycler (Bio-Rad, Hercules, CA). Specifically, in an 8-strip PCR tube, reactions were allowed to proceed on the thermal annealing ramp one at a time while the other tubes were held for longer periods of time at the initial 65 °C step. Once the desired temperature gradient was achieved across the block (10 °C or 12 °C range), all of the wells then decreased in temperature at the same rate of 3 h/°C following the steps of our standard annealing protocol. The folding reaction was then stopped when the desired average temperature was reached. For example, with a final average temperature of 50 °C and range of 10 °C, the first tube would be cooled at 3 h/°C until reaching 45 °C, and the last tube would spend additional time at 65 °C and then be cooled at 3 h/°C to a final temperature of 55 °C. The extended time at 65 °C for subsequent wells did not cause any noticeable effects on folding results. Examples of these partial fold analyses are shown in figure S29 for multiple slider versions.

After the desired incubation time at the final temperature, folding reactions were mixed with viscous gel loading dye (New England BioLabs, Ipswich, MA) to halt the folding while still in the heating block and then immediately pipetted into the well of an agarose gel. Samples were imaged by TEM after gel purification. Agarose gels were prepared and run as described in [21], and TEM grids were prepared as previously described.

Results

Controlling sequence of component self-assembly

We demonstrate our ordered assembly concept in figure 2. We modified the staple design of our DNA origami slider (figure S13) to program the inside track to form before the tube (figure 2(a)) by adapting an approach of Dunn *et al* [41]. We used partial folding ramps, shown in figures 2(b) and S29, to verify that this structure indeed forms in two steps, first the track, which then positions the remaining scaffold to later form the tube concentrically around the track as discussed subsequently. The partial folding ramps were paused part way through the annealing ramp after reaching temperatures ranging from 60 °C to 48 °C. Depositing these warm samples directly into reaction-inhibiting gel loading dye and then running them through an agarose gel we see a shift as the temperature decreases, suggesting that the two components are assembling in the desired sequential

manner. This was verified by TEM images, also in figure 2(b). The schematics at the top of figures 2(b)–(d) are 2D design maps from the DNA origami design software cadnano [42]. The left component in these schematics corresponds to the track and the right component corresponds to the tube. The color of the staple strands in each component represents the relative annealing temperature of the staples, red meaning high annealing temperature, or the component that will form first, and blue signifying a lower annealing temperature, or the component that will form second.

The bar graphs in figures 2(b)–(d) show the binding energy of the highest affinity staples in each component, calculated based on the model of Dunn *et al* [41]. Their model considers the free energy change from formation of the DNA duplex as well as the change in entropy due to formation of a loop in the single-stranded DNA scaffold. Since we are only interested in identifying which component is likely to assemble first, we only considered interactions between individual staples and the scaffold. The histograms show the binding energy for the 30 staples with lowest free energy of binding (i.e. most favorable binding).

The configuration shown in figure 2(b) where the track forms first results in ∼40% of properly formed sliders, meaning the two components are concentrically arranged. Figure 2(c) shows results of a slider where both components' staples have the lower melting temperature, like a standard DNA origami structure. This design resulted in misfolded sliders with ∼0% of the sliders with the two pieces concentrically folded. Instead, the tube was formed outside of the track, resulting in a poorly formed slider, which cannot perform constrained linear motion. Figure 2(d) shows a version of the slider where the tube was programmed to form first, also resulting in misfolded sliders with ∼0% proper folding. These results were measured through negative-stained TEM images (figures S22–S24). These three versions of the slider all have two 86 nt long scaffold connections between the backstop and tube and two more 96 nt scaffold connections between the opposite end of the tube and the end of the track.

In addition to this approach of adjusting staple thermodynamics by staple design, we also explored the use of staple concentration as a means to direct order of folding. For the version where neither component was modified for high annealing temperatures (figures 2(c) and S10), we tested variations in the staple concentration as a means for controlling the order of folding. With a constant concentration of tube staples at 40 nM, we increased the track staple concentration from 200 up to 400 nM. Increasing the track staple concentration resulted in a higher percentage of concentrically formed structures (figure S30), likely due to faster binding kinetics and slightly higher annealing temperatures for the track. Although the effect was minor in this range of staple concentrations, these results suggest that the experimental conditions of self-assembly can also be used as a means to influence DNA origami folding pathways as has recently been demonstrated for a 2D origami structure [43].

Controlling topology of intermediate states to fold concentric structures

Our staple design approach to direct initial folding of the track component (figure 2(b)) resulted in an improvement from 0% to 40% properly formed (concentric components) sliders. This approach forces an intermediate folding state where just the track is assembled. We hypothesized that this intermediate state templates the folding of the tube component by controlling the arrangement of the remaining scaffold. In the current design, the remaining scaffold, which ultimately forms the tube, comprises two scaffold loops connected from the backstop to the opposite end of the track. Each of these loops makes up half the tube. With this design it is possible for both scaffold loops to displace to one side of the track during folding so the tube can still fold external to the track as illustrated in figure 3(a). We pursued two approaches to increase the probability of concentric folding, both designed to better constrain the scaffold loops around the track at the intermediate state. First, we increased the number of intermediate state scaffold loops that ultimately make up the tube. Figure 3(b) shows one design where six intermediate state scaffold loops were used to form the tube, which resulted in 100% concentric structures, indicating that improving the constraint of scaffold loops around the track prior to folding indeed results in better yield. As a separate control, we designed a structure where the intermediate state scaffold loop connects only to the backstop. This loop can easily displace to the side of the track during folding, and hence this design yielded 0% concentric structures (figure 3(c)). We further tested a design with four intermediate state scaffold loops. The yield of concentric structures for 2-, 4-, and 6-loop designs is summarized in figure 3(d) (top). Each of these designs has the same 86 nt length of single-stranded scaffold DNA connecting the tube and the backstop in the final structure.

To test whether adding scaffold connections between the track and tube without changing their length would hinder motion, we measured extensional distributions of each slider structure (figure 3(d), middle). These translational probability distributions were converted into energy landscapes following our prior work

Figure 3. Directing folding pathways by designing intermediate state scaffold topology. (a) Designing an intermediate state where the two scaffold loops (each ultimately making up half the tube) are pinned between the backstop and the end of the track results in a distribution of concentric and non-concentric structures. (b) Keeping the scaffold pinned across the track and adding more connections prevents the scaffold from fluctuating away from the track and forces the tube to always form in the concentric state. (c) This design includes an intermediate state where the track is formed with one scaffold loop attached to the backstop that will form the tube. For this design the scaffold loop can easily tilt to the side of the track and the tube forms exclusively non-concentrically. (d) Analyzing the effect of the number of connections between the tube and the track, we see a significant increase in properly arranged structures with more connections. Scaffold connections in these three cases have the same length, defined by the length between the tube and backstop in the final structure (86 nt). Extension distributions were measured from TEM images and free energy landscapes were calculated assuming a Boltzmann distribution. This data shows a slight shift towards smaller extensions likely due to the additional entropic springs. These designs are available in figures S1, S4, and S7. (e) The effect of connection length between the backstop and tube was studied to show that shorter connections result in slightly higher folding efficiency. Extension distributions show that decreasing connections length also decreases the range of motion. These designs all have two scaffold connections between the outer tube and inner track at either end of the tube (figures S7–S9). Further analysis is available in figures S31–S33.

[28]. The energy landscapes show that additional connections result in slightly decreased range of motion. Hence, in this case there is a tradeoff between improving yield and range of motion.

We further tested to see if reducing the length of the scaffold loops by reducing the length of the final connections would also improve the yield of concentric structures. As shown in figure 3(e), there is a clear increase in concentrically formed sliders as the connections get shorter, but this effect is weaker than the effect from changing the number of loops used to fold the tube. In addition, decreasing the length of connections limits the range of motion as expected. In total, we tested nine combinations of number and length of intermediate state loops. Figure 3 illustrates the primary trends observed. Additional TEM images, yield of concentric structures, and length distributions are shown for all of the designs tested in supplementary figures S14–S22, S25, and S31–S33.
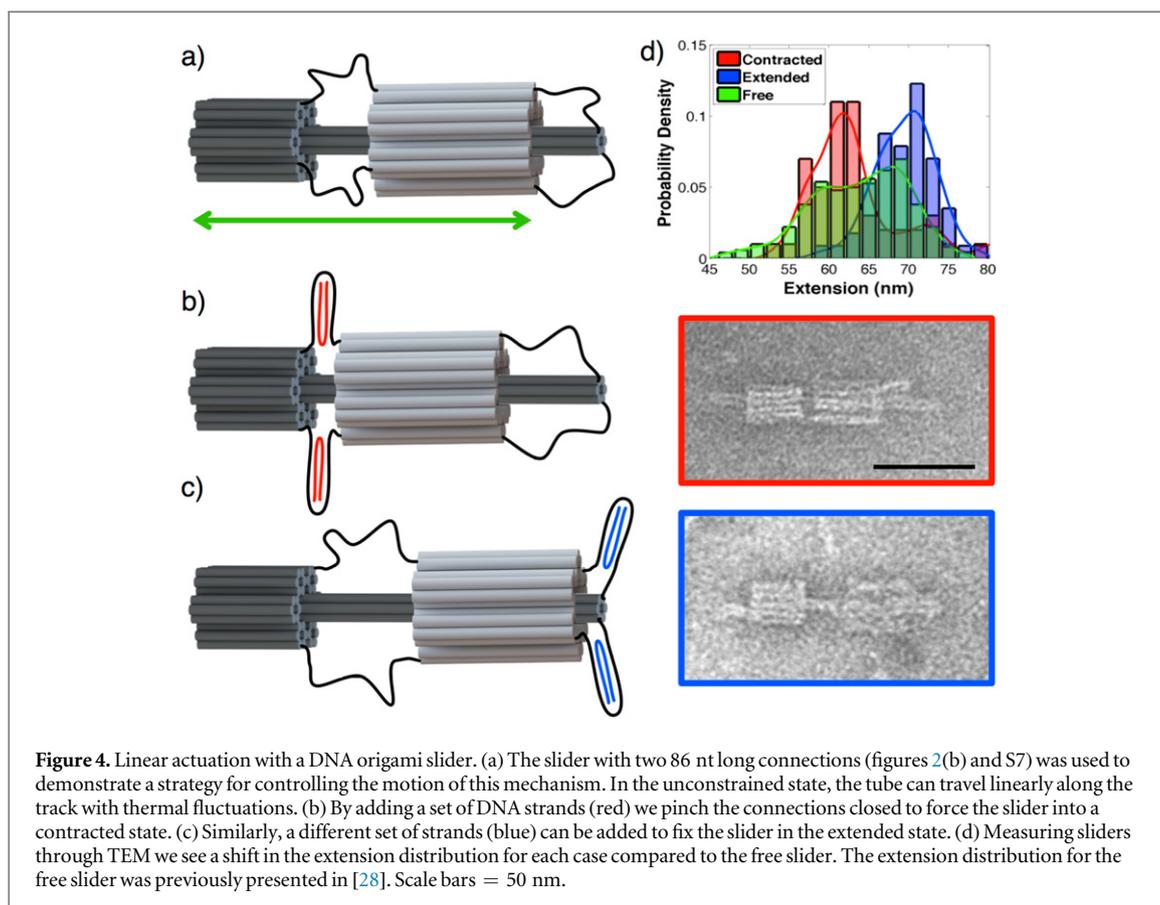
Figure 4. Linear actuation with a DNA origami slider. (a) The slider with two 86 nt long connections (figures 2(b) and S7) was used to demonstrate a strategy for controlling the motion of this mechanism. In the unconstrained state, the tube can travel linearly along the track with thermal fluctuations. (b) By adding a set of DNA strands (red) we pinch the connections closed to force the slider into a contracted state. (c) Similarly, a different set of strands (blue) can be added to fix the slider in the extended state. (d) Measuring sliders through TEM we see a shift in the extension distribution for each case compared to the free slider. The extension distribution for the free slider was previously presented in [28]. Scale bars = 50 nm.

Actuating linear motion of the slider

A properly formed DNA slider serves as a linear joint useful in engineering mechanisms as shown in our previous work [28]. The slider was initially presented with freely fluctuating motion due to thermal energy. Here we present a method for controlling the linear motion using DNA inputs. We measured the extension of the slider as the distance from the back of the backstop to the far end of the tube. By adding short single-stranded DNA strands designed to pinch together the scaffold connections on each end of the tube (figure 4), we can control the configuration of the sliders. As shown in figure 4(b), a set of strands was added to close the middle connections, resulting in sliders with the tube contracted. This yields a clear shift of extension lengths in the distributions of figure 4(d). Similarly, in figure 4(c) strands were added to pinch the connections on the front end of the slider, resulting in mostly extended sliders also evident in the linear distributions in figure 4(d). Sliders in these actuated configurations still have some flexibility due to some single-stranded DNA slack left between the two components. The contracted case has 6 nt of slack and the extended case has 14 nt. Some slack is necessary to traverse the distance between the two attachment points. Additional TEM images are available in figures S26–S27.

Discussion

This work demonstrates the ability to program the order of assembly for multi-component structures. We adapted the method of Dunn *et al* [41], who introduced the ability to guide folding of a flat rectangular structure into distinct folded states by biasing a particular trajectory among competing pathways. Here we expand this method to control sequence of assembly for multi-component structures. Specifically, we show removing a small number of cross-overs to increase the local thermal stability allows selection of which component folds first. This approach is easily adapted to existing DNA origami designs, and the modified staples can easily be substituted in or out without having to redesign or repurchase the staples comprising most of the structure. While removing cross-overs likely affects local mechanical stability, only a few modifications are needed, and here we did not observe a noticeable affect on the overall structure. For some cases where mechanical stiffness is critical, alternative methods such as re-arranging scaffold architecture to control looping energies or placing regions with high GC-content at specific locations could be explored. These approaches, however, are not amenable to easy substitution of staple strands.

We have further demonstrated that control of the scaffold topology in intermediate states is a means to direct folding pathways of subsequent components. Specifically, we exploit folding of the first component to template folding of the second component. A similar concept has previously been used with DNA origami to template the assembly of strands to form tubes [44] or fill internal cavities [45]. Here we use the initial folding of the track to pre-position the scaffold concentrically around the track. The degree of constraint and flexibility of the scaffold loops then determines selection between the concentric and non-concentric pathways. This also provides an interesting approach to select distributions of final states, as was the case here for either two or four scaffold connections. Aside from allowing selection of a folding pathway, this folding from pre-arranged scaffold topologies could also serve as a potential means to improve yield or speed up self-assembly. In general, the consideration of design at multiple states along the folding pathway can open possibilities for other structures with complex topology such as internal and external parts or perhaps intertwined strands or knots within larger DNA origami structures, as has been demonstrated for smaller strand assemblies [46].

Furthermore, the ability to select a folding pathway at an intermediate state could allow for the design of kinetically trapped states. In this case, the energy required to stretch the scaffold linkers would favor the concentric state, while electrostatic repulsions between the track and tube and configurational entropy of the slider would favor the non-concentric state. Our results show that selecting the concentric assembly requires careful control of the folding pathway, namely forcing the track to fold first and pre-arranging the tube scaffold around the track. In the absence of programming the folding pathway, the slider reaches the non-concentric state, suggesting it is likely the lower energy state. Regardless, once the track is assembled in either the concentric or non-concentric state, the energy barrier to cross between the two assembly states is too large to achieve via thermal fluctuations. For our concentric structures, we never observed conformations where the base of the tube was close to reaching the end of the track. It is also possible that folding in either state could create topological barriers to switching between the concentric and non-concentric state.

The studies presented here have shown novel methods for programming sequential folding of DNA origami components during the self-assembly process, controlling the topology of such components, and actuating linear motion. Controlling linear motion with a device like the DNA slider offers new potential for fabricating and actuating DNA nanomachines using a traditional engineering machine design approach [28]. These strategies expand the possibilities for complex DNA nanostructure design allowing for the assembly of intricate multi-part devices and the ability to arrange components in kinetically trapped energy states. Furthermore, given recent advances in computational modeling of DNA origami nanostructures [47–50] and of their self-assembly [40], our results can provide both motivation and a guide to improve understanding and modeling of DNA origami dynamics and self-assembly, which will continue to enhance design of structure and function. As the field of structural DNA nanotechnology expands and nanostructure designs become increasingly complicated, considerations of folding pathways and intermediate states will offer opportunities to create new types of complex nanodevices with dynamic components.

Acknowledgments

References

[1] Boothroyd G 1994 Product design for manufacture and assembly *Comput. Aided Des.* **26** 505–20
[2] Boothroyd G, Dewhurst P and Knight W A 2010 *Product Design for Manufacture and Assembly* (Boca Raton, FL: CRC Press)
[3] Whitney D E 2004 *Mechanical Assemblies: their Design, Manufacture, and role in Product Development* (Oxford: Oxford University Press)
[4] Mao Y, Yu K, Isakov M S, Wu J, Dunn M L and Jerry Qi H 2015 Sequential self-folding structures by 3D printed digital shape memory polymers *Sci. Rep.* **5** 13616
[5] Hawkes E *et al* 2010 Programmable matter by folding *Proc. Natl Acad. Sci. USA* **107** 12441–5
[6] Felton S, Tolley M, Demaine E, Rus D and Wood R 2014 Applied origami. A method for building self-folding machines *Science* **345** 644–6
[7] Bhatia D, Mehtab S, Krishnan R, Indi S S, Basu A and Krishnan Y 2009 Icosahedral DNA nanocapsules by modular assembly *Angew. Chem.* **48** 4134–7
[8] Iinuma R, Ke Y, Jungmann R, Schlichthaerle T, Woehrstein J B and Yin P 2014 Polyhedra self-assembled from DNA tripods and characterized with 3D DNA-PAINT *Science* **344** 65–9
[9] He Y, Ye T *et al* 2008 Hierarchical self-assembly of DNA into symmetric supramolecular polyhedra *Nature* **452** 198–201

[10] Jungmann R, Scheible M, Kuzyk A, Pardatscher G, Castro C E and Simmel F C 2011 DNA origami-based nanoribbons: assembly, length distribution, and twist *Nanotechnology* **22** 275301

[11] Dietz H, Douglas S M and Shih W M 2009 Folding DNA into twisted and curved nanoscale shapes *Science* **325** 725–30

[12] Haorong C, Tae-Gon C, Jing P and Jong Hyun C 2013 Hierarchically assembled DNA origami tubules with reconfigurable chirality *Nanotechnology* **24** 435601

[13] Knudsen J B *et al* 2015 Routing of individual polymers in designed patterns *Nat. Nanotechnol.* **10** 892–8

[14] Winfree E, Liu F, Wenzler L A and Seeman N C 1998 Design and self-assembly of two-dimensional DNA crystals *Nature* **394** 539–44

[15] Liu H, He Y, Ribbe A E and Mao C 2005 Two-dimensional (2D) DNA crystals assembled from two DNA strands *Biomacromolecules* **6** 2943–5

[16] Liu W, Zhong H, Wang R and Seeman N C 2011 Crystalline two-dimensional DNA-origami arrays *Angew. Chem.* **50** 264–7

[17] Zheng J *et al* 2009 From molecular to macroscopic via the rational design of a self-assembled 3D DNA crystal *Nature* **461** 74–7

[18] Cademartiri L and Bishop K J 2015 Programmable self-assembly *Nat. Mater.* **14** 2–9

[19] Rothemund P W 2006 Folding DNA to create nanoscale shapes and patterns *Nature* **440** 297–302

[20] Douglas S M, Dietz H, Liedl T, Hogberg B, Graf F and Shih W M 2009 Self-assembly of DNA into nanoscale three-dimensional shapes *Nature* **459** 414–8

[21] Castro C E *et al* 2011 A primer to scaffolded DNA origami *Nat. Methods* **8** 221–9

[22] Torring T, Voigt N V, Nangreave J, Yan H and Gothelf K V 2011 DNA origami: a quantum leap for self-assembly of complex structures *Chem. Soc. Rev.* **40** 5636–46

[23] Linko V and Dietz H 2013 The enabled state of DNA nanotechnology *Curr. Opin. Biotechnol.* **24** 555–61

[24] Sacca B and Niemeyer C M 2012 DNA origami: the art of folding DNA *Angew. Chem.* **51** 58–66

[25] Andersen E S *et al* 2009 Self-assembly of a nanoscale DNA box with a controllable lid *Nature* **459** 73–6

[26] Han D, Pal S, Nangreave J, Deng Z, Liu Y and Yan H 2011 DNA origami with complex curvatures in three-dimensional space *Science* **332** 342–6

[27] Castro C E, Su H J, Marras A E, Zhou L and Johnson J 2015 Mechanical design of DNA nanostructures *Nanoscale* **7** 5913–21

[28] Marras A E, Zhou L, Su H J and Castro C E 2015 Programmable motion of DNA origami mechanisms *Proc. Natl Acad. Sci. USA* **112** 713–8

[29] Zhou L, Marras A E, Su H J and Castro C E 2014 DNA origami compliant nanostructures with tunable mechanical properties *ACS Nano* **8** 27–34

[30] Zhou L, Marras A E, Su H J and Castro C E 2015 Direct design of an energy landscape with bistable DNA origami mechanisms *Nano Lett.* **15** 1815–21

[31] Douglas S M, Bachelet I and Church G M 2012 A logic-gated nanorobot for targeted transport of molecular payloads *Science* **335** 831–4

[32] Kuzyk A, Schreiber R, Zhang H, Govorov A O, Liedl T and Liu N 2014 Reconfigurable 3D plasmonic metamolecules *Nat. Mater.* **13** 862–6

[33] Gerling T, Wagenbauer K F, Neuner A M and Dietz H 2015 Dynamic DNA devices and assemblies formed by shape-complementary, non-base pairing 3D components *Science* **347** 1446–52

[34] Liedl T, Hogberg B, Tytell J, Ingber D E and Shih W M 2010 Self-assembly of three-dimensional prestressed tensegrity structures from DNA *Nat. Nanotechnol.* **5** 520–4

[35] Zhang F *et al* 2015 Complex wireframe DNA origami nanostructures with multi-arm junction vertices *Nat. Nanotechnol.* **10** 779–84

[36] Shih W M and Lin C 2010 Knitting complex weaves with DNA origami *Curr. Opin. Struct. Biol.* **20** 276–82

[37] Ketterer P, Willner E M and Dietz H 2016 Nanoscale rotary apparatus formed from tight-fitting 3D DNA components *Sci. Adv.* **2** e1501209

[38] Arbona J M, Aime J P and Elezgaray J 2013 Cooperativity in the annealing of DNA origamis *J. Chem. Phys.* **138** 015105

[39] Sobczak J P, Martin T G, Gerling T and Dietz H 2012 Rapid folding of DNA into nanoscale shapes at constant temperature *Science* **338** 1458–61

[40] Snodin B E, Romano F, Rovigatti L, Ouldridge T E, Louis A A and Doye J P 2016 Direct simulation of the self-assembly of a small DNA origami *ACS Nano* **10** 1724–37

[41] Dunn K E, Dannenberg F, Ouldridge T E, Kwiatkowska M, Turberfield A J and Bath J 2015 Guiding the folding pathway of DNA origami *Nature* **525** 82–6

[42] Douglas S M, Marblestone A H, Teerapittayanon S, Vazquez A, Church G M and Shih W M 2009 Rapid prototyping of 3D DNA-origami shapes with caDNAno *Nucleic Acids Res.* **37** 5001–6

[43] Lee Tin Wah J, David C, Rudiuk S, Baigl D and Estevez-Torres A 2016 Observing and Controlling the Folding Pathway of DNA Origami at the Nanoscale *ACS nano* **10** 1978–87

[44] Mohammed A M and Schulman R 2013 Directing self-assembly of DNA nanotubes using programmable seeds *Nano Lett.* **13** 4006–13

[45] Li W, Yang Y, Jiang S, Yan H and Liu Y 2014 Controlled nucleation and growth of DNA tile arrays within prescribed DNA origami frames and their dynamics *J. Am. Chem. Soc.* **136** 3724–7

[46] Ciengshin T, Sha R and Seeman N C 2011 Automatic molecular weaving prototyped by using single-stranded DNA *Angew. Chem.* **50** 4419–22

[47] Yoo J and Aksimentiev A 2013 In situ structure and dynamics of DNA origami determined through molecular dynamics simulations *Proc. Natl Acad. Sci. USA* **110** 20099–104

[48] Doye J P *et al* 2013 Coarse-graining DNA for simulations of DNA nanotechnology *Phys. Chem. Chem. Phys.* **15** 20395–414

[49] Pan K, Kim D-N, Zhang F, Adendorff M R, Yan H and Bathe M 2014 Lattice-free prediction of three-dimensional structure of programmed DNA assemblies *Nat. Commun.* **5** 5578

[50] Kim D N, Kilchherr F, Dietz H and Bathe M 2012 Quantitative prediction of 3D solution shape and flexibility of nucleic acid nanostructures *Nucleic Acids Res.* **40** 2862–8